INSTITUTE OF PHYSICS PUBLISHING PLASMA SOURCES SCIENCE AND TECHNOLOGY
Plasma Sources Sci. Technol. **14** (2005) 293–300 doi:10.1088/0963-0252/14/2/010

Transport coefficients for electrons in argon in crossed electric and magnetic rf fields

Z M Raspopović[1], S Dujko[1], T Makabe[2] and Z Lj Petrović[1]

[1] Institute of Physics, University of Belgrade, PO Box 68, 11080 Zemun, Belgrade, Serbia and Montenegro
[2] Department of Electronics and Electrical Engineering, Keio University, 3-14-1 Hiyoshi, Yokohama 223-8522, Japan

Received 30 November 2004
Published 8 March 2005
Online at stacks.iop.org/PSST/14/293

Abstract
Monte Carlo simulations of electron transport have been performed in crossed electric and magnetic rf fields in argon. It was found that a magnetic field strongly affects electron transport, producing complex behaviour of the transport coefficients that cannot be predicted on the basis of dc field theory. In particular, it is important that a magnetic field, if it has sufficiently high amplitude, allows energy gain from the electric field only over a brief period of time, which leads to a pulse of directed motion and consequently to cyclotron oscillations being imprinted on the transport coefficients. Furthermore, this may lead to negative diffusion. The behaviour of drift velocities is also interesting, with a linear (sawtooth) dependence for the perpendicular drift velocity and bursts of drift for the longitudinal. Non-conservative effects are, on the other hand, reduced by the increasing magnetic field.

1. Introduction

A detailed knowledge of electron transport coefficients as well as a full understanding of the kinetic phenomena that may occur in rf fields are two basic requirements in modelling of electron kinetics in low-temperature rf plasmas. On the other hand, the kinetics of electrons develops on the shortest time scale and is therefore one of the critical components in plasma modelling. Since modelling of electron transport is almost exclusively based on swarm theory, it is highly desirable to apply the most advanced techniques of electron swarm physics in order to provide the necessary data and further understanding. In particular, one needs to apply techniques that do not depend on hydrodynamic expansion, since electron transport in critical regions of low-temperature rf plasmas will be non-local and also may not be relaxed in time. There are two main techniques in electron swarm physics that may fulfil this requirement: the kinetic Boltzmann equation [1] and Monte Carlo simulation. Very strict tests that have been developed in swarm physics should also be applied to electron kinetics codes that are part of complex plasma modelling systems.

In practice, only the dc data for drift velocities, diffusion coefficients and ionization and attachment rate coefficients are used in fluid codes as input parameters [2]. Even the dc $\boldsymbol{E} \times \boldsymbol{B}$ data are not employed because of the complexity. Electron transport coefficients obtained under conditions of rf electric fields are required for modelling of plasma applications such as capacitively coupled rf plasmas (CCPs) [2, 3]. Crossed electric and magnetic rf fields are the input data necessary for models of plasma reactors that also involve magnetic fields such as inductively coupled plasmas (ICPs) [4], rf magnetrons and magnetically enhanced CCPs [5]. In the kinetic or Monte Carlo segment of the hybrid codes that uses the cross sections [6], the application of dc swarm data to establish good sets of cross sections is necessary, yet it is not certain whether in practice most cross sections have been obtained using the swarm procedure. Therefore, in addition to the dc swarm data, one needs both $\boldsymbol{E} \times \boldsymbol{B}$ data and time resolved data. While it may be difficult to incorporate time resolved transport data [7] in fluid and hybrid codes, it is certainly important to check what kind of kinetic phenomena may be expected [8, 9] and then to test whether the plasma codes may be able to predict them. For example, a recent extension of a standard plasma model

by Kushner and coworkers [7, 10, 11] to include $\boldsymbol{E} \times \boldsymbol{B}$ effects and time resolved kinetics has led to a better understanding of the power transfer to ICPs which is consistent with studies by Makabe and coworkers [12] in a different geometry.

Several studies of electron transport in gases under swarm conditions in crossed dc electric and magnetic fields have been carried out in model gases [13–17] and in real gases [18–23]. However, there are only a few published papers that have considered time resolved electron transport in crossed rf electric and magnetic fields [8, 9, 24–27]. In this paper, we study the behaviour of electron transport coefficients in crossed electric and magnetic rf fields in pure argon using a Monte Carlo simulation technique. A preliminary presentation of these data was given in [27].

A big part of the motivation to study electron transport in crossed electric and magnetic fields originates from the development of particle detectors and associated swarm studies that provide the corresponding databases [28, 29]. On the other hand, as discussed above, studies of time resolved electron transport in crossed electric and magnetic fields are required for modelling, design and control of rf plasmas. Argon is one of the gases most commonly used in plasma processing both pure [30] and in mixtures [31], and so there is considerable interest in studying the electron kinetics of this gas. Ness and Makabe [22] have presented a detailed investigation of electron transport in crossed dc electric and magnetic fields in order to form a database of transport data for fluid models of argon magnetron discharges. Our investigation in rf fields is a logical extension of their work. However, it is not an attempt to describe the complete set of data for electron transport in argon in rf fields, but to discuss the basic features of electron transport in argon in crossed rf electric and magnetic fields. Consequently we compare these results with basic results arising from a detailed investigation of electron transport in model gases such as the Reid ramp model [25]. This paper should illustrate the applicability of the Monte Carlo technique, and in case the complete data are required for some application, the technique should be incorporated into the model. The review of kinetic phenomena serves as a basis for making a decision whether these phenomena will affect the basic physics in a particular situation.

2. Monte Carlo method

We have used our time resolved Monte Carlo simulation code that has been described in great detail in some of our previous publications [8, 17, 24]. The code has been verified for a number of benchmarks [17] which prove the accuracy and the correctness of the code. In addition, the code has been cross-checked with a Boltzmann equation solution of White and Robson, and excellent agreement has been found even for the most complex phenomena [32, 39].

The electron swarm is assumed to develop in an infinite gas under uniform fields. It is also assumed that the electron density is sufficiently small so that Coulomb interactions between the particles and shielding of the field are negligible. All calculations were performed for zero gas temperature, but for the conditions of calculations the effects of gas temperature would be negligible.

The Monte Carlo code used in this work follows a large number of electrons (typically 10^4–10^6) over small time steps allowing them to relax to a quasi-stationary mode. The probability of scattering an electron with energy ε in the time interval $(t, t + \mathrm{d}t)$ may be written as

$$p(t) = \nu_{\mathrm{T}}(\varepsilon(t)) \exp\left[-\int_0^t \nu_{\mathrm{T}}(\varepsilon(t))\mathrm{d}t\right],$$

where $\nu_{\mathrm{T}}(\varepsilon(t))$ is the time dependent total collision frequency. We have used the integration technique for numerical solution of the above equation where the small time steps are determined by the minimum of the three relevant time constants (mean collision time, period of the field and cyclotron period for $\boldsymbol{E} \times \boldsymbol{B}$). The chosen time constant has been divided by a large number (20–100). At the same time the period of the field is always divided by 100, and these moments are used to sample the transport coefficients. We have used the integration technique instead of the traditional null-collision technique since it has an advantage for time (and space) varying fields.

The formulae used to sample transport coefficients were taken from [13, 14, 17]. In order to represent non-conservative processes (attachment and ionization) in a correct manner, we distinguish between bulk and flux transport coefficients. The rate coefficients (including the ionization) may be determined by counting the appropriate events and normalizing the count by the time step and number of electrons. Another option for determining the ionization rate coefficient is to follow the spatial or temporal growth of the number of electrons. Both procedures agree very well. We have not determined rates and transport data from sampled EEDF as these calculations may be affected by the choice of formulae used for integration.

In final calculations we used the simplest form of the cross sections with two cross sections for excitation with a threshold energy of 11.6 eV and 11.8 eV, respectively, and an ionization cross section with a threshold energy of 15.6 eV [22]. Those were shown to predict very accurately all the results by comparing the data with predictions based on a much more detailed set from Hayashi [33].

We chose a limited set of parameters that are typical for practical devices: 1 Torr pressure and 100 MHz frequency (this is equivalent to 0.1 Torr and 10 MHz). The amplitude of the applied electric field is 100 and 1000 Td ($1\,\mathrm{Td} = 10^{-21}\,\mathrm{V\,m^2}$), while the amplitudes of the applied magnetic field are 0, 10, 100, 1000 and 5000 Hx ($1\,\mathrm{Hx} = 10^{-27}\,\mathrm{T\,m^3}$). The values of E/N and B/N refer to the amplitude. The phase difference between the electric and magnetic fields is 90°, which corresponds to the conditions found in ICPs. The electric field has a sinusoidal time dependence, while the magnetic field follows a cosine one. In the figures we show the time dependence of the fields and transport coefficients during one period. As magnetic and electric fields are perpendicular, we use them to denote the axes of the coordinate system with the addition of the third, $\boldsymbol{E} \times \boldsymbol{B}$, axis.

In our simulations we have followed typically 1×10^5 electrons. First, we allowed them to relax to quasi-stationary conditions and then we performed averaging over several periods. We made sure that sampling was carried out for uncorrelated conditions of each electron by allowing the collision frequency to be at least as high and usually much

higher than the sampling frequency. As mentioned above, sampling was carried out at fixed times uncorrelated to the moments of collisions.

3. Results and discussion

3.1. Time dependence of transport coefficients as a function of B/N

First we show (figure 1) the results for the mean energy (for 100 Td, 1 Torr and 100 MHz). As can be seen, for low values of B/N (0, 10, 100 Hx) there is no significant cooling of the rf electron swarm. However, further increasing of B/N leads to a more significant decrease in the mean energy and cooling of the electron swarm. We may observe that the symmetric profile of the mean energy at low values of B/N becomes asymmetric and triangular at high B/N with a fast increase and slower decrease. At high values of B/N, electrons cannot follow the electric field due to the fact that their trajectories are 'frozen' around the magnetic field lines. In other words, as B/N increases, the cyclotron frequency will be larger and electrons will complete large parts or whole cyclotron orbits before colliding with neutral particles of the background gas. The net result is a decreasing of the mean energy which may be expected from the dc studies. The fast increase in the energy is due to a very brief period when the magnetic field is zero and electrons are free to accelerate, and the long decay occurs due to collisions over the period when the magnetic field reduces the chances of electrons gaining energy. This effect reduces the delay between the mean energy and electric field that is observable at low B/N values.

Figure 2 shows the behaviour of the longitudinal component of the drift velocity (i.e. the drift velocity in the $\boldsymbol{E}$ direction). At low values of B/N there are no significant changes in the drift velocity or mean energy. Although there is no visible decrease in the drift velocity in the $\boldsymbol{E}$ direction (v_E) at such low B/N values, it is possible to detect a significant effect of the increase in the drift velocity in the $\boldsymbol{E} \times \boldsymbol{B}$ direction ($v_{E\times B}$) as shown in figure 3. For a higher B/N value, the maximum value of the drift velocity remains pretty much the same (actually it is even higher than for the zero magnetic field), but the region where it is high is narrower and narrower. One should observe the difference in the time dependence before and after the magnetic field passes through zero. The increase is more gradual and without undulations, while the decrease is sudden and followed by pronounced oscillations. Clearly the difference is in the mean energy and especially in the additional directed motion of electrons due to the effect of the electric field.

One may claim that the perpendicular drift velocity is the most sensitive coefficient to B/N (as well as the corresponding component of the diffusion tensor, $ND_{E\times B}$) as may be expected. We may also observe that both components of the drift velocity lose symmetry as B/N increases, and evidently the mean value is not zero. At the highest values of B/N, strong oscillations are induced for both components of the drift velocity, but for the $\boldsymbol{E} \times \boldsymbol{B}$ component, an almost linear drift velocity dependence (sawtooth) is observed with superimposed oscillations. Due to the chaotic nature of the electron motion, the oscillations are not just pure cyclotron motion but the imprint of that motion on the group properties of electrons. In other words as they begin their rotations, the electrons have a whole range of initial conditions in all directions and may suffer collisions some time during the cycle. Yet it does mean that the cyclotron frequency becomes equal or higher than the collision frequency. The oscillations are the highest after the intake of the energy (and consequently of the directed motion) from the field, and they decay as the

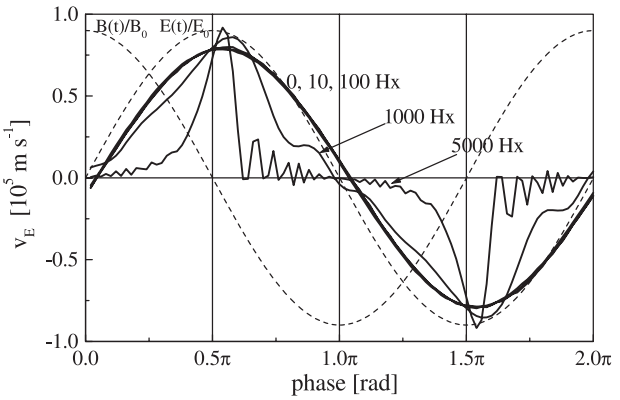

Figure 2. Time dependence of the longitudinal drift velocity as a function of B/N. The frequency of the applied electric field is 100 MHz at $E/N = 100$ Td.

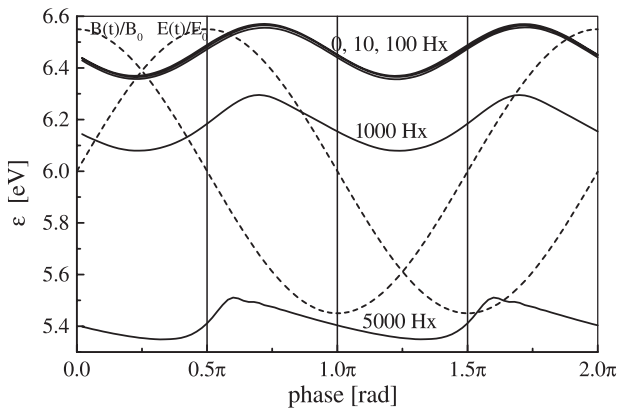

Figure 1. Time dependence of the mean energy as a function of B/N. The frequency of the applied electric field is 100 MHz at $E/N = 100$ Td.

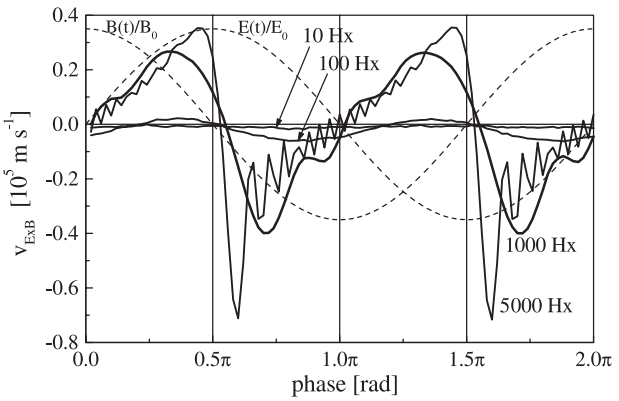

Figure 3. Time dependence of the perpendicular velocity as a function of B/N. The frequency of the applied electric field is 100 MHz at $E/N = 100$ Td.

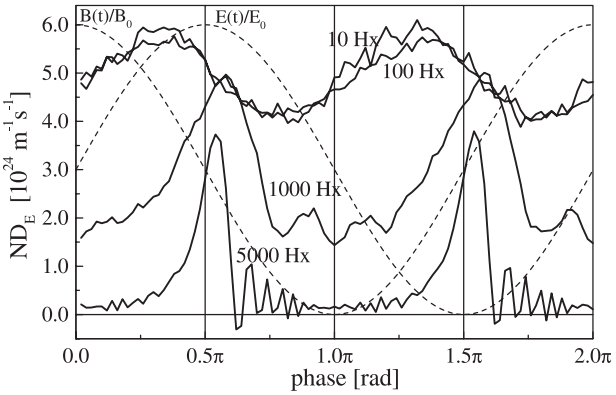

Figure 4. Time dependence of the longitudinal component of the diffusion tensor (ND_E) as a function of B/N. The frequency of the applied electric field is 100 MHz at $E/N = 100$ Td.

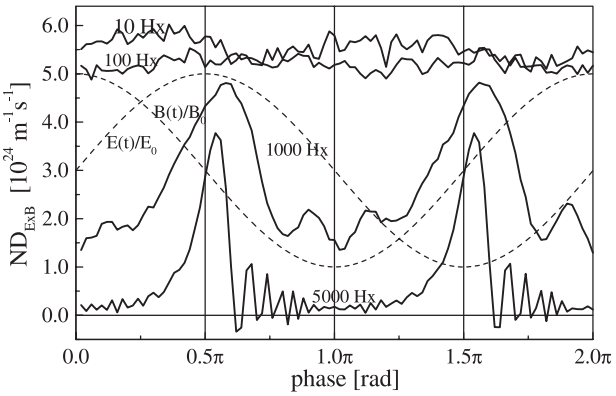

Figure 5. Time dependence of the transverse component of the diffusion tensor ($ND_{E\times B}$) as a function of B/N. The frequency of the applied electric field is 100 MHz at $E/N = 100$ Td.

energy decays due to dissipation in collisions. For the $\boldsymbol{E}\times\boldsymbol{B}$ component, we observe that even the change in the sign of the electric field does not affect the $\boldsymbol{E}\times\boldsymbol{B}$ drift velocity; only the sign changes, but the development (linear dependence and decay of oscillations) is continuous.

Recent plasma models rely on diffusion coefficients that are constant in both space and time and are isotropic. Also, we are not aware of the models that take advantage of the $\boldsymbol{E}\times\boldsymbol{B}$ transport data, though some kinetic or hybrid codes may take the $\boldsymbol{E}\times\boldsymbol{B}$ effects into account. It is obvious that such approximations may not be adequate even from the viewpoint of dc data. We have therefore studied the behaviour of the components of the diffusion tensor in crossed electric and magnetic rf fields.

In figure 4 we show the time development of the longitudinal component of the diffusion tensor, ND_E, and in figure 5 we show the behaviour of the transverse ($\boldsymbol{E}\times\boldsymbol{B}$) component of the diffusion tensor, $ND_{E\times B}$. One particularly interesting feature of ND_E is that it shows signs of anomalous diffusion. This kinetic phenomenon was observed in time varying electric fields as well as for crossed electric and magnetic rf fields for Reid's ramp model [34, 35]. Following the initial studies of anomalous diffusion, the effect was also indicated for numerous real gases by approximate solution of the time dependent Boltzmann equation [36]. Anomalous diffusion occurs when the field changes sign, and it leads to

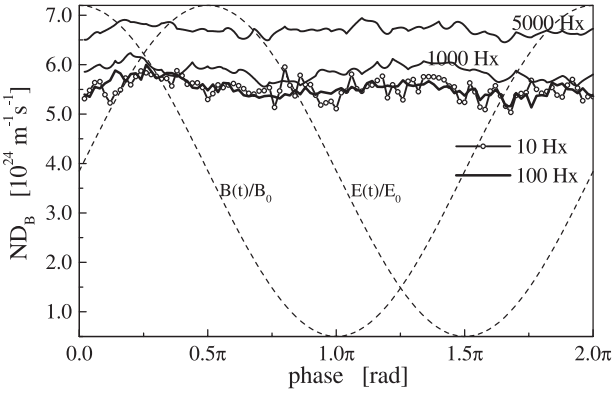

Figure 6. Time dependence of the transverse component of the diffusion tensor (ND_B) as a function of B/N. The frequency of the applied electric field is 100 MHz at $E/N = 100$ Td.

a situation where the ND_E component has a peak at the point where we expect it has to go through a minimum, when the electric field goes through the zero value. As can be seen, the ND_E component does not change much at low values of B/N. As B/N increases, the trajectories of the electrons become frozen and diffusion is allowed only at times when the magnetic field goes through zero. At the highest values of B/N, the phase of the diffusion maxima is shifted to the phase of the zero magnetic fields. Also, at the highest value of B/N, strong oscillations are induced due to cyclotron motion. One can hardly speak of anomalous diffusion at this point since it cannot be associated with the change in sign of the electric field. Yet the transition to this mode is continuous from the initial transients at low B/N values.

In the case of $ND_{E\times B}$, at low values of B/N, the diffusion coefficient has a very small modulation, while at high values of B/N it begins to behave like the ND_E component of the diffusion tensor. In addition, it has all the features of the anomalous diffusion [24]. As mentioned above, both components have strong oscillations and occasionally the diffusion coefficients become negative. While the negative value of a diffusion coefficient may be interesting in principle from the kinetic theory viewpoint, it is clear that the magnetic field induced cyclotron motion is the cause.

In figure 6 we show the behaviour of the diffusion coefficient in the direction of the magnetic field, ND_B. Perhaps the most striking feature of the profile of the ND_B is the enhancement in amplitude as the magnetic field increases. This is in contrast with the behaviour of ND_B for the ramp model where ND_B decreases as the magnetic field increases [24, 32]. The explanation was found in the different dependences of the diffusion coefficients on the mean energy for the two gases.

3.2. Time dependence of transport coefficients as a function of E/N

In this section we show the basic features of the time dependence of the transport coefficients as a function of the reduced electric field (E/N-amplitude). In figure 7 we show the time dependence of the mean energy as a function of E/N. At the highest value of E/N (1000 Td) the mean energy has much more modulation as compared with the lower values of E/N. This is caused by the fact that at high values of E/N,

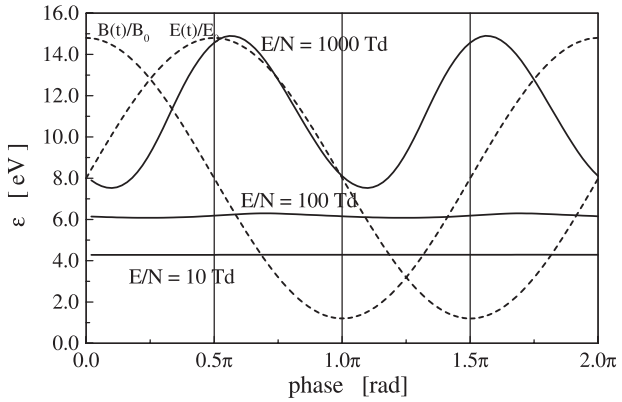

Figure 7. Time dependence of the mean energy as a function of E/N. The frequency of the applied electric field is 100 MHz at $B/N = 1000$ Hx.

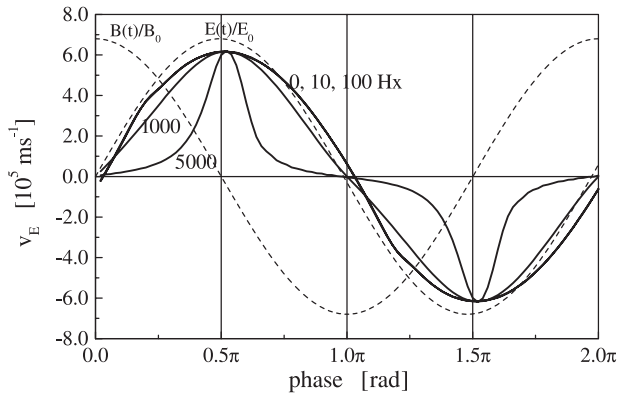

Figure 8. Time dependence of the longitudinal drift velocity as a function of B/N. The frequency of the applied electric field is 100 MHz at $E/N = 1000$ Td.

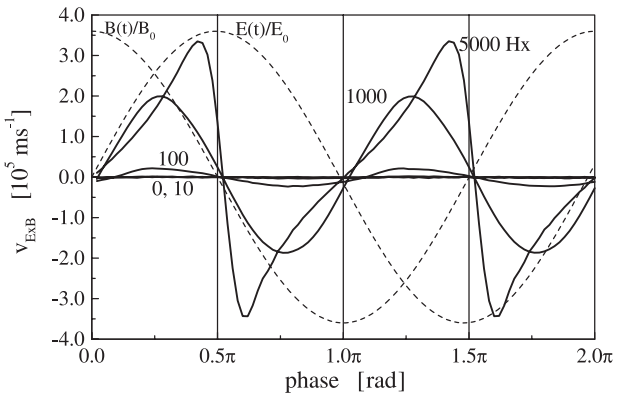

Figure 9. Time dependence of the perpendicular drift velocity as a function of B/N. The frequency of the applied electric field is 100 MHz at $E/N = 100$ Td.

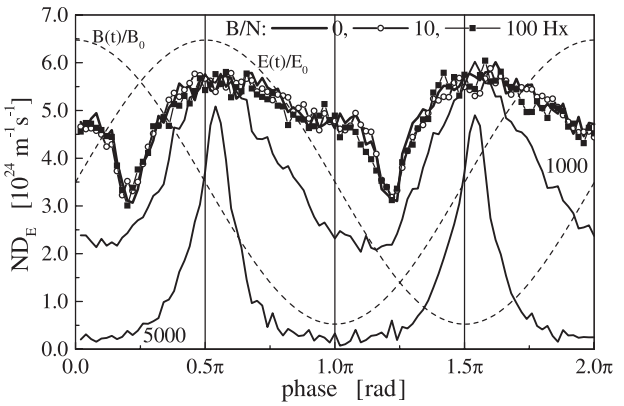

Figure 10. Time dependence of the longitudinal component of the diffusion tensor (ND_E) as a function of B/N. The frequency of the applied electric field is 100 MHz at $E/N = 1000$ Td.

electrons are capable of losing their energy more efficiently in inelastic processes. At the lowest value of the reduced electric field shown here, $E/N = 10$ Td, the amplitude of the mean energy modulation is almost impossible to observe at the scale from 0 to 16 eV, while for $E/N = 100$ Td it is very small.

In figure 8 we show the time dependence of the longitudinal component of the drift velocity (v_E) at $E/N = 1000$ Td, which appears to be similar to the results at $E/N = 100$ Td shown in figure 2. In contrast to figure 2, the profiles at $B/N = 1000$ and 5000 Hx are almost symmetric and more narrow, while the peak value does not change as the magnetic field increases. Also, it is very important to note that at $E/N = 1000$ Td the drift velocity does not show any signs of oscillations. All these observations, together with the higher modulation of the mean energy shown in figure 7, indicate that at higher $E/N = 1000$ Td the electric field is still strong enough to give full acceleration to the electrons and consequently the collision frequency and mean energy are not affected strongly by the magnetic field.

It is interesting to check what happens to the perpendicular drift velocity, $v_{E\times B}$, at $E/N = 1000$ Td, and the results for various magnetic fields are shown in figure 9. At $B/N = 1000$ Hx, the profile is still almost sinusoidal, while at $E/N = 100$ Td the profile at $B/N = 1000$ Hx was linear (sawtooth) with superimposed oscillations as can be seen in figure 3. At $E/N = 1000$ Td, the sawtooth profile is established only at $B/N = 5000$ Hx but without superimposed oscillations. These results may be again associated with the relative ratio of the collision and cyclotron frequencies, and so for this value of the reduced electric field one would need much higher reduced magnetic fields to induce oscillations. The linear part of the sawtooth waveform, however, consists of two different slopes, indicating perhaps sensitivity of that slope to the mean electron energy which is much more modulated. At $E/N = 1000$ Td, the drift velocity is symmetric in the positive and negative directions unlike the results for $E/N = 100$ Td shown in figure 3.

The time dependence of the longitudinal diffusion coefficient at $E/N = 1000$ Td for various magnetic fields is shown in figure 10, and these results should be compared with the data for the smaller reduced field shown in figure 4. At low B/N values, the profile is asymmetric with a fast increase and a slow decrease. We can also observe that there is a minimum at the same phase where ND_E peaks at $E/N = 100$ Td. In addition, at $E/N = 1000$ Td, ND_E peaks at the same phase that corresponds to the maximum of the electric field for all reduced magnetic fields. On the other hand, at $E/N = 100$ Td the phases of the maxima of the longitudinal diffusion are shifted with the increasing magnetic field towards the phase of zero magnetic field. Thus, at the higher reduced electric field

the effect of the magnetic field is less pronounced, and it is the electric field and the energy dependence of the diffusion that are the key in explanation of the time dependence of the longitudinal diffusion. From the local minimum, one may expect that longitudinal diffusion is reduced significantly for a range of mean energies, which may explain the fact that the maximum of diffusion at 100 Td does not occur for the maximum reduced electric field. Only at the highest value of the reduced magnetic field ($B/N = 5000$ Hx) does diffusion become very small (practically zero) except at the times when the magnetic field goes through the zero. In any case, the longitudinal diffusion coefficient waveforms at the highest value of E/N can be regarded as anomalous [24, 34–36].

The time dependence of the transverse diffusion coefficient along the $\boldsymbol{E} \times \boldsymbol{B}$ direction at $E/N = 1000$ Td is similar to that of the longitudinal diffusion. At the higher values of B/N it follows the same time dependence as ND_E and has all the features of anomalous diffusion [24]. However, at the highest values of B/N the shapes of the time dependence are more symmetric and rounded with respect to the shapes at $E/N = 100$ Td.

Finally, in figure 11 we show the time dependence of the ionization rate coefficient as a function of both E/N (100 and 1000 Td) and B/N (0 and 5000 Hx). However, due to the large differences between the results for 100 and 1000 Td, we use the logarithmic scale. As E/N increases from 100 to 1000 Td, the ionization rate coefficient increases by more than two orders of magnitude. At low E/N values, there are only a few electrons that are capable of reaching the energy necessary for ionization.

In the case of 100 Td, the ionization coefficient is not affected much by magnetic fields up to 1000 Hx. All other rate coefficients have a time dependence similar to that of the ionization coefficients.

The mean energy easily approaches 6 eV even at reduced electric fields as low as $E/N = 100$ Td due to the lack of inelastic processes below 11 eV. However, the tail of the EEDF drops down very rapidly with the energy due to the effect of inelastic collisions. Thus the efficiency of ionization may be much smaller than that in a molecular gas at the same mean energy. As E/N increases, there is a rapid increase in the tail of the EEDF and consequently an increase in the ionization rate coefficient, while all other characteristics of an electron swarm do not change markedly (for example the mean energy). Therefore, as there is an increase in the number of electrons in the energy zone above the thresholds for excitation and ionization, the energy exchange is much more efficient, leading to an increase in the modulation of the mean energy.

On the other hand, at $E/N = 1000$ Td the time profile of the ionization coefficient is apparently narrower (if plotted on a linear scale) as compared with the profile at $E/N = 100$ Td, especially at high B/N values. In other words, the peak values at 1000 Td are almost unaffected by the magnetic field, while at $E/N = 100$ Td there is an almost uniform decrease in the ionization coefficient profile at all phases, as B/N increases.

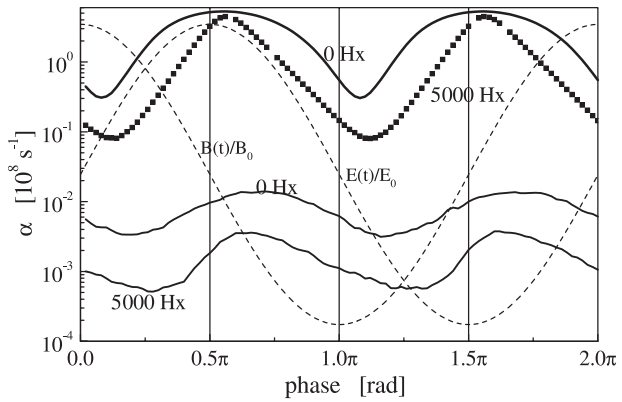

Figure 11. Time dependence of the ionization rate coefficient as a function of E/N (100 Td is shown by thin lines and 1000 Td by bold lines) and B/N (0 and 5000 Hx). The frequency of the applied electric field is 100 MHz.

3.3. Non-conservative transport

We now turn our attention to non-conservative processes and their effect on the electron transport coefficients. In figures 12(*a*) and (*b*) we show the time dependence of the flux and bulk values of both the components of the drift velocity for (*a*) zero magnetic field and for (*b*) $B/N = 1000$ Hx at 1000 Td and 100 MHz. Since the effect of non-conservative collisions is not significant at 100 Td, we show the result of our simulations only at 1000 Td. For zero magnetic fields, the effect of non-conservative processes (the effect of ionization) is considerable. Both components have sinusoidal profiles, but the bulk component of the drift velocity is much larger. However, for a magnetic field with an amplitude of 1000 Hx, the distinction between bulk and flux drift velocities is much smaller. Actually, if we take a careful look, we can see that the bulk component is reduced and becomes more similar to the flux component as the magnetic field is increased. The reduction in the non-conservative effect (i.e. the difference between bulk and flux transport properties) with an increase in the magnetic field is mainly due to reduction of the mean energy and consequently of the ionization coefficient. At the same time, for $B/N = 1000$ Hx there is a component of the drift velocity in the $\boldsymbol{E} \times \boldsymbol{B}$ direction. Figure 12(*b*) clearly shows that there is almost no significant distinction between the bulk and flux components of the $\boldsymbol{E} \times \boldsymbol{B}$ component of the drift velocity. If there is any effect in any case it leads to a reduction in the drift velocity, which is the opposite of the behaviour of the longitudinal drift velocity.

This result demands a further investigation since there is a strong effect of the anomalous diffusion in the same direction. In other words, the $\boldsymbol{E} \times \boldsymbol{B}$ component of the force appears to be acting in the same way as an electric field itself. However, the lack of the effect of non-conservative collisions shows that this similarity is not complete. A discussion of the non-conservative effects in an rf electric field was made by White *et al* [37] and in both pure electric and crossed electric and magnetic fields by Sakadžić and Petrović [38].

4. Conclusion

In this paper we have presented the most important properties of the electron transport coefficients in crossed electric and magnetic rf fields in argon obtained using Monte Carlo simulations. We are not aware of any other similar data to compare our results with. The simulation conditions have

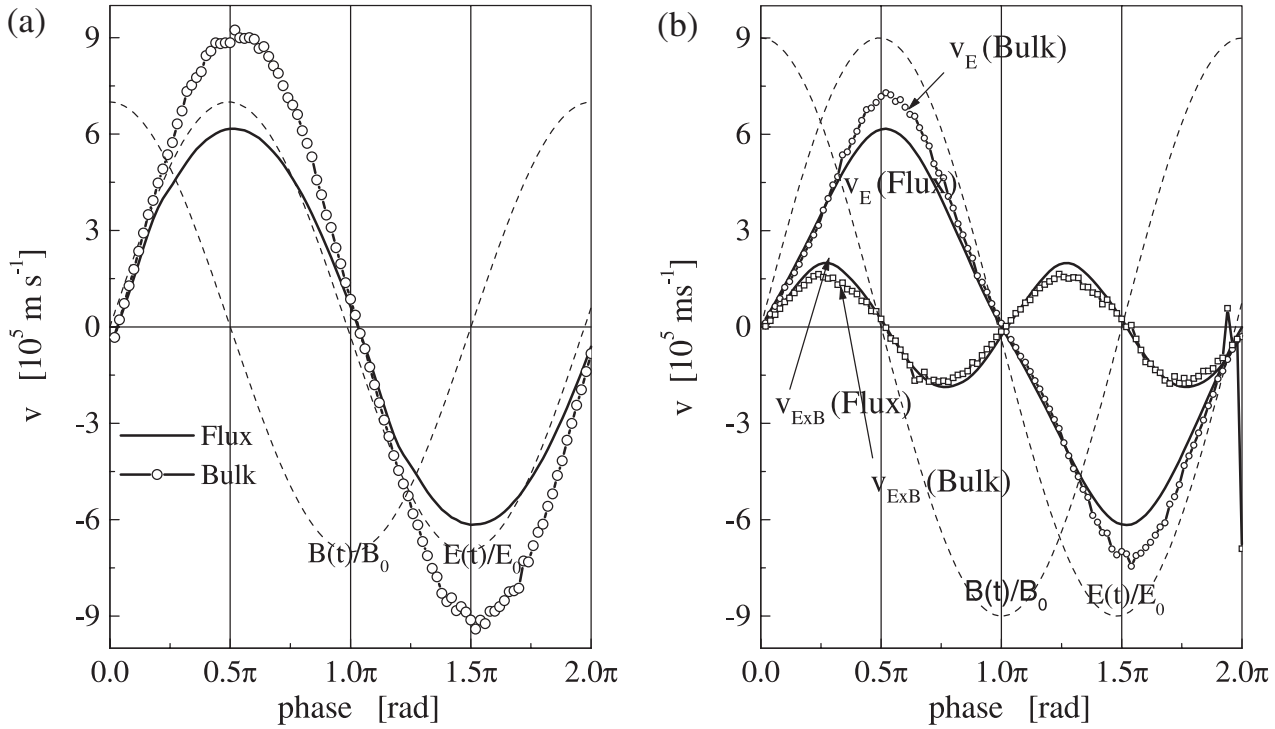

Figure 12. Time dependence of the bulk and flux drift velocities in the $\boldsymbol{E}$ and $\boldsymbol{E} \times \boldsymbol{B}$ directions at 1000 Td and 100 MHz for (*a*) $B/N = 0$ Hx and (*b*) $B/N = 1000$ Hx.

been carefully selected in order to check how a magnetic field controls the electron motion in realistic conditions such as those found in ICP reactors.

Our results show that the magnetic field strongly affects electron transport and causes complex behaviour of the transport coefficients. The mean energy is reduced with increasing amplitude of the rf B/N above 100 Hx, and at very high B/N it changes shape to sawtooth-like (triangular) with a fast increase during the period when the magnetic field is small and a slow decay for the remainder of the period. Small undulations of the mean energy may be associated with much larger oscillations in other transport properties. Oscillations appear to be induced by a pulse of directed motion given to the swarm during the period when the magnetic field is zero when electrons are free to move (and be accelerated) along the electric field. The longitudinal drift velocity has a narrow peak at high E/N values that is even higher than that for the drift velocity in a purely electric field. Its shape is asymmetric, with stronger oscillations after the peak. The time dependence for the perpendicular ($\boldsymbol{E} \times \boldsymbol{B}$) drift velocity is linear even though the sign changes. The change in sign does not seem to affect the gradual decay of oscillations.

The observed oscillations are not numerical in nature. They have been confirmed both by varying the time steps in our procedure and also by a completely different method—numerical solution of the time dependent Boltzmann equation [39]. The two codes agreed quantitatively in all details. As mentioned in the text, even though the random velocities are much larger than the directed velocity, each electron makes parts of cyclotron orbits which are imprinted on the properties of the collective motion of the ensemble. At larger E/N values, the collisional frequencies are much higher (as compared with the cyclotron frequency) and the relative contribution of the cyclotron motion (i.e. the oscillations) is not observed.

The diffusion coefficients have the same features as expected, anomalous diffusion and transition of the $\boldsymbol{E} \times \boldsymbol{B}$ component from the behaviour of the transverse to the behaviour similar to the longitudinal component of the tensor [24]; in other words, anomalous diffusion is induced in this component even for small fields. Yet at higher fields both components are non-zero almost throughout the period, with a peak at times when the magnetic field passes through zero, followed by oscillations that even allow negative values of the diffusion coefficient for brief periods of time.

The ionization coefficient gives an indication of the effect of the magnetic field on high energy electrons. Thus it is strongly affected by the magnetic field, showing that in particular the magnetic field does not allow the population of the highest energies in the energy distribution function to develop. As a result, magnetic fields decrease the non-conservative effects. The development of the transport coefficient and the corresponding behaviour of the energy distribution functions do not allow easy representation of these phenomena using dc data or simplified formulae.

Not surprisingly, rf transport in argon has numerous features that cannot be extrapolated from the dc transport coefficients and may be difficult to include in fluid models of low temperature plasmas.

Acknowledgment

This work was supported by the Ministry of Science project 1478. The authors are also grateful to R D White and R E Robson for useful discussions.

References

[1] Kumar K, Skullerud H R and Robson R E 1980 *Aust. J. Phys.* **33** 343

[2] Nakano N, Shimura N, Petrović Z Lj and Makabe T 1994 *Phys. Rev.* E **49** 4455

[3] Kushner M J 1985 *J. Appl. Phys.* **58** 4024–31
Graves D B and Kushner M J 2003 *J. Vac. Sci. Technol.* A **21** 152–6

[4] Makabe T 2001 *Advances in Atomic, Molecular and Optical Physics* vol 44, ed M Kimura and Y Itikawa (San Diego, CA: Academic) pp 127–54

[5] Shidoji E, Ness K and Makabe T 2001 *Vacuum* **60** 299
Kushner M J 2003 *J. Appl. Phys.* **94** 1436–47

[6] Shimada T, Nakamura Y, Petrović Z Lj and Makabe T 2003 *J. Phys. D: Appl. Phys.* **36** 1936
Rauf S and Kushner M J 1999 *J. Vac. Sci. Technol.* A **17** 704–12

[7] Sankaran A and Kushner M J 2002 *J. Appl. Phys.* **92** 736–48

[8] Petrović Z Lj, Raspopović Z M, Dujko S and Makabe T 2002 *Advances in Low Temperature Plasmas* ed T Makabe (Amsterdam: Elsevier) pp 1–25
Petrović Z Lj, Raspopović Z M, Dujko S and Makabe T 2002 *Appl. Surf. Sci.* **192** 1–25

[9] White R D, Ness K F and Robson R E 2002 *Advances in Low Temperature Plasmas* ed T Makabe (Amsterdam: Elsevier) pp 26–49
White R D, Ness K F and Robson R E 2002 *Appl. Surf. Sci.* **192** 26–49

[10] Vasenkov A V and Kushner M J 2003 *J. Appl. Phys*. **94** 5522

[11] Vasenkov A V and Kushner M J 2003 *J. Appl. Phys*. **94** 2223

[12] Tadokoro M, Hirata H, Nakano N, Petrović Z Lj and Makabe T 1998 *Phys. Rev.* E **57** R43–6

[13] White R D, Brennan M J and Ness K F 1997 *J. Phys. D: Appl. Phys.* **30** 810

[14] Nolan A M, Brennan M J, Ness K F and Wedding A B 1997 *J. Phys. D: Appl. Phys*. **30** 2865

[15] Ness K F 1994 *J. Phys. D: Appl. Phys.* **30** 810

[16] Ikuta N and Sugai Y J 1989 *J. Phys. Soc. Japan* **56** 115

[17] Raspopović Z M, Sakadžić S, Bzenić S A and Petrović Z Lj 1999 *IEEE Trans. Plasma Sci.* **27** 1241

[18] Brenan M J, Garvie A M and Kelly L J 1990 *Aust. J. Phys.* **43** 27

[19] Raju G R G and Dincer M S 1990 *IEEE Trans. Plasma Sci.* **18** 819

[20] Liu J and Raju G R G 1991 *J. Phys. D: Appl. Phys.* **25** 465

[21] Dincer M S 1993 *J. Phys. D: Appl. Phys.* **26** 1427

[22] Ness K F and Makabe T 2000 *Phys. Rev.* E **62** 4083

[23] Dujko S, Raspopović Z M and Petrović Z Lj 2002 *Proc. XVI ESCAMPIG and V ICRP (Grenoble, France, 14–18 July 2002)* ed N Sadeghi and H Sugai, pp 101–2
Dujko S, Raspopović Z M and Petrović Z Lj 2003 *Proc. the 5th General Conf. of the Balkan Physical Union (Vrnjačka Banja, Serbia & Montenegro, 25–29 August 2003)* ed S Jokić *et al* , pp 1017–22

[24] Raspopović Z M, Sakadžić S, Petrović Z Lj and Makabe T 2000 *J. Phys. D: Appl. Phys.* **33** 1298

[25] Raspopović Z M 2000 *Proc. Invited Lectures of the XX SPIG (Zlatibor, Yugoslavia, 26–30 September 2000)* ed N Konjević *et al* (Belgrade: SFIN Institute of Physics) pp 129–44

[26] Dujko S, Raspopović Z M and Petrović Z Lj 2003 *Proc. 56th GEC (San Francisco, California, 21–24 October 2003) Bull. Am. Phys. Soc.* **48** XF15

[27] Raspopović Z M, Sakadžić S, Petrović Z Lj 1999 *Proc. 52nd GEC (Norfolk, Virginia, 5–8 October 1999)* ETP3 *Bull. Am. Phys. Soc.* **44** 29
Raspopović Z M, Sakadžić S, Petrović Z Lj and Makabe T 2000 *Proc. 15th ESCAMPIG Miskolc-Lillafured* ed Z Donko *et al* pp 160–1

[28] Kunst T, Götz B and Schmidt B 1993 *Nucl. Instrum. Methods* A **324** 127–40

[29] Becker U, Dinner R, Fortunato E, Kirchner J, Rosera K and Uchida Y 1999 *Nucl. Instrum. Methods* A **421** 54–9

[30] Tochikubo F, Petrović Z Lj, Kakuta S, Nakano N and Makabe T 1994 *Japan. J. Appl. Phys.* **33** 4271
Tadokoro M, Hirata H, Nakano N, Petrović Z Lj and Makabe T 1998 *Phys. Rev.* E **58** 7823–30

[31] Hioki K, Hirata H, Matsumura S, Petrović Z Lj and Makabe T 2000 *J. Vac. Sci. Technol*. **18** 864–72
Kurihara M, Petrović Z Lj and Makabe T 2000 *J. Phys. D: Appl. Phys.* **33** 2146–53

[32] Raspopović Z M, Dujko S, Petrović Z Lj, White R D, Ness K F and Robson R E 2003 unpublished

[33] Hayashi M 1992 personal communication

[34] White R D, Robson R E and Ness K F 1995 *Aust. J. Phys.* **48** 925

[35] Maeda K, Makabe T, Nakano N, Bzenić S and Petrović Z Lj 1997 *Phys. Rev.* E **55** 5901

[36] Aleksandrov N L, Dyatko N A and Kochetov I V 1996 *Russ. Fiz. Plazmi* **22** 88–92
Aleksandrov N L, Dyatko N A and Kochetov I V 1996 *Plasma Phys. Rep.* **22** 82 (Engl. Transl.)

[37] White R D, Robson R E and Ness K F 1999 *Phys. Rev.* E **60** 7457–72

[38] Raspopović Z M, Sakadžić S, Benić S and Petrović Z Lj 1998 *Proc. 51st GEC (Gaseous Electronics Conf.) and 4th ICRP (International Conf. on Reactive Plasmas) (Maui, 1998) Bull. Am. Phys. Soc.* **43** 1413 (BM1 4)
Sakadžić S, Petrović Z Lj, Raspopović Z M and Petrović N 1999 *Proc. Int. Symp. on Electron–Molecule Collisions and Swarms (Tokyo, 18–20 July 1999)* ed Y Hatano *et al* pp 115–16
Sakadžić S and Petrović Z Lj 1999 unpublished

[39] Dujko S, Raspopović Z M, Petrović Z Lj, White R D and Robson R E 2004 *Proc. 22nd SPIG (Tara, Serbia and Montenegro, 23–27 August 2004)* ed Lj Hadžijevski (Belgrade: INN Vinča) pp 109–13